MCB
Journals.ASM.org

The General Transcription Factor TAF7 Is Essential for Embryonic Development but Not Essential for the Survival or Differentiation of Mature T Cells

Anne Gegonne,[a] Xuguang Tai,[a] Jinghui Zhang,[b] Gang Wu,[b] Jianjian Zhu,[c] Aki Yoshimoto,[c] Jeffrey Hanson,[d] Constance Cultraro,[b] Qing-Rong Chen,[e] Terry Guinter,[a] Zhihui Yang,[b] Karen Hathcock,[a] Alfred Singer,[a] Jaime Rodriguez-Canales,[d] Lino Tessarollo,[f] Susan Mackem,[c] Daoud Meerzaman,[b] Ken Buetow,[b] and Dinah S. Singer[a]

Experimental Immunology Branch,[a] Laboratory of Population Genetics,[b] and Laboratory of Pathology,[d] Center for Cancer Research, National Cancer Institute, National Institutes of Health, Bethesda, Maryland, USA; Cancer and Developmental Biology Laboratory[c] and Mouse Cancer Genetics Program,[f] Center for Cancer Research, National Cancer Institute, Frederick, Maryland, USA; and Center for Biomedical Informatics and Information Technology, National Cancer Institute, Rockville, Maryland, USA[e]

TAF7, a component of the TFIID complex that nucleates the assembly of transcription preinitiation complexes, also independently interacts with and regulates the enzymatic activities of other transcription factors, including P-TEFb, TFIIH, and CIITA, ensuring an orderly progression in transcription initiation. Since not all TAFs are required in terminally differentiated cells, we examined the essentiality of TAF7 in cells at different developmental stages *in vivo*. Germ line disruption of the TAF7 gene is embryonic lethal between 3.5 and 5.5 days postcoitus. Mouse embryonic fibroblasts with TAF7 deleted cease transcription globally and stop proliferating. In contrast, whereas TAF7 is essential for the differentiation and proliferation of immature thymocytes, it is not required for subsequent, proliferation-independent differentiation of lineage committed thymocytes or for their egress into the periphery. TAF7 deletion in peripheral CD4 T cells affects only a small number of transcripts. However, T cells with TAF7 deleted are not able to undergo activation and expansion in response to antigenic stimuli. These findings suggest that TAF7 is essential for proliferation but not for proliferation-independent differentiation.

Initiation of transcription by RNA polymerase II (Pol II) requires the assembly of the transcription machinery at the promoter (33). For many promoters, the binding of the TFIID complex to the promoter is the first step in the assembly of a transcription preinitiation complex. TFIID is a multiprotein complex consisting of the TATA-binding protein (TBP) associated with at least a dozen TBP-associated factors, TAFs (8). When originally identified, the TAFs were assumed to serve exclusively as components of TFIID. However, more recently, TAFs have been isolated in SAGA transcription complexes, independent of either TBP or TFIID (17, 28, 38).

Furthermore, whereas TAFs were originally thought to function simply as accessory proteins involved in either the stabilization of TFIID or of TFIID-transcriptional regulation, it is now clear that they actively contribute to cell specific transcriptional regulation (for review, see references 21, 26, and 27). It has been reported that during myogenesis, expression of all TAFs and TBP are terminated, with the exception of TAF3 which functions with TRF3 to mediate myocyte transcription (12). During early embryonic development, TAF10 and TAF8 are essential for the survival of blastocyst inner cells but not of trophoblast cells (25, 36). TAF8 acts as a positive regulator of adipogenesis (18); TAF10 is required for the acquisition of skin barrier function in the fetal epidermis (20).

Among the TAFs, TAF7 is the only one demonstrated to interact with and regulate the enzymatic activities of transcription factors required for transcription initiation and elongation. Within the TFIID complex, TAF7 binds to TAF1 and inhibits the TAF1 acetyltransferase (AT) activity required for transcription initiation (15). TAF7 also binds to and inhibits the kinase activities of TFIIH/CDK7 and P-TEFb/CDK9, factors necessary for transcription initiation and elongation, respectively (13). Based on these observations, we have proposed that TAF7 plays a key role in transcription, functioning as a check point regulator that modulates the three different enzymatic activities required for initiation and elongation of transcription (13, 14).

However, the role of TAF7 in transcription may not be universal. Although a temperature sensitive mutation of TAF7 leads to growth arrest in yeast, only 24% of the genes require TAF7 (32). Similarly, in differentiated human 293 kidney cells, only 65% of the genes depend on TAF7 for their expression (3). Only one study has addressed the *in vivo* role of TAF7: in zebrafish, germ line deletion of TAF7 is lethal at 5 days of development (1, 2, 16). Taken together, these findings suggest that cellular requirements for TAFs, and TAF7 in particular, may be related to the stage of development or cellular differentiation.

Therefore, we undertook to determine whether the cellular requirements for TAF7 changed during differentiation and development *in vivo*. We find that TAF7 is essential for mouse embryonic development and for maintenance of established cultures of mouse embryonic fibroblasts (MEFs). TAF7 is also essential for the differentiation of immature thymic precursors that undergo massive proliferation during their differentiation. In sharp contrast, TAF7 is not required for the subsequent proliferation-independent differentiation of lineage committed thymocytes and

Received 20 September 2011 **Returned for modification** 13 October 2011
Accepted 4 March 2012
Published ahead of print 12 March 2012
Address correspondence to Dinah S. Singer, singerd@mail.nih.gov.

doi:10.1128/MCB.06305-11

their egress into the periphery. However, TAF7-deficient peripheral T cells are not able to undergo activation and expansion in response to antigenic stimuli, although only a small number of transcripts is affected by TAF7 deletion. We conclude that TAF7 plays a critical role in transcription in cells that undergo proliferation but that its role is more restricted in nonproliferating differentiated cells.

MATERIALS AND METHODS

Generation of TAF7$^{+/-}$ mice. The Cre-LoxP system was used to generate a targeted TAF7 allele (TAF7t) (Fig. 1A) (10, 23), in which a LoxP site was introduced within the first intron of the gene and a cassette containing a neomycin resistance, flanked on each side by LoxP and Frt recombinase sites, was introduced in the noncoding sequence of the second exon. Southern blot analyses revealed that the LoxP site and the *neo* cassette were correctly inserted by homologous recombination in 9 of 110 *neo*-resistant ES clones (data not shown), of which one was selected to generate recombinant mice. Southern blot analyses performed on tail DNA from mice heterozygous for the TAF7t allele confirmed the presence of the inserted LoxP sites and *neo* cassette (Fig. 1B). The action of the Cre recombinase on the TAF7t allele was expected to delete the entire LoxP-flanked ("floxed") sequence, including the *neo* cassette and part of the second TAF7 exon that contains the complete sequence coding for the TAF7 protein, thereby generating a TAF7-null (TAF7^{-}) allele. Crossing TAF7$^{+/t}$ animals with mice carrying a β-actin Cre transgene, which expresses the Cre recombinase in all cells, including germ cells, generated TAF7$^{+/-}$ animals carrying the disrupted allele, as confirmed by PCR and Southern blotting (Fig. 1). The β-actin Cre transgene was eliminated from TAF7$^{+/-}$ offspring by breeding with C57BL/6 mice.

Generation of TAF7$^{f/f}$ mice. To generate TAF7$^{+/f}$ mice, TAF7$^{+/t}$ mice were bred with mice expressing the Flpe recombinase under the control of the β-actin promoter. TAF7$^{+/f}$ offspring were then bred with C57BL/6 mice to produce TAF7$^{+/f}$ mice which do not carry the β-actin *flpe* transgene. Homozygous TAF7$^{f/f}$ mice were derived by intercrossing TAF7$^{+/f}$ mice.

Generation of either TAF7$^{f/-}$ LCK-Cre$^{+/-}$ mice or TAF7$^{f/-}$ E8$_{III}$-Cre$^{+/-}$ mice and analysis of the thymocytes. TAF7$^{+/-}$ mice were bred with mice expressing the Cre recombinase under the control of either the LCK proximal promoter (Taconic) or the CD8 enhancer III (E8$_{III}$ [29]). Either TAF7$^{+/-}$ LCK-Cre$^{+/-}$ offspring or TAF7$^{+/-}$ E8$_{III}$-Cre$^{+/-}$ offspring were then bred with TAF7$^{f/f}$ mice to produce TAF7$^{f/-}$ LCK-Cre$^{+/-}$ (TAF7$^{f/-}$ LCK-Cre) and TAF7$^{f/-}$ E8$_{III}$-Cre$^{+/-}$ (TAF7$^{f/-}$ E8$_{III}$-Cre) mice, respectively. Cells were prepared from the thymus, spleens, and lymph nodes, counted, and assessed for CD4 and CD8 surface protein expression by flow cytometry using a FACSVantage apparatus (BD Biosciences).

Oligonucleotide sets used for genotyping mice and quantitative PCR. The following oligonucleotide pairs were used: TAF7, ATTCCAGCT CTTCCTGCAAA and ATGAAAGGCAAGCTCCAAGA; Slc25a2, GAGA CAGATCCCAGCAAAGC and GGACTCTCGACCACTCTTGC; knockout fragment, GAAGGCAAGTTCTCAATGAAAGGG and CGAAGAGT TCGTTCACTCCC; Flox fragment, GAAGGCAAGTTCTCAATGAA AGGG and GTATGAAAACCTGTGTCCTGGTCTG; Cre transgene, CG ATGCAACGAGTGATGAGG and GCATTGCTGTCACTTGGTCGT; and Flpe transgene, CACTGATATTGTAAGTAGTTTGC and CATCCA AATATACAAGTGGATCG.

Recovery of blastocysts at 3.5 days postcoitus (dpc) from TAF7$^{+/-}$ intercrosses. Four-week-old TAF7$^{+/-}$ females were induced to superovulate by injection with gestyl FSH (gonadotropin), followed by HCG (chorionic gonadotropin), and then bred with TAF7$^{+/-}$ males. The plug was examined the following day, and the blastocysts were recovered 3 days later by flushing the uterus with M2 medium. Collected blastocysts were individually maintained in culture for 2 days in M16 medium. The DNA was purified using a QIAamp DNA micro kit from Qiagen, and the blastocysts were genotyped by PCR using Hot Start TaKaRa polymerase and the TAF7 and Slc25a2 oligonucleotide sets.

Genotyping of the 5.5-dpc embryos. Females from TAF7$^{+/-}$ intercrosses were sacrificed at 5.5 dpc, and their uteri were collected, embedded, and sectioned on slides. Embryos were detected by hematoxylin and eosin staining and then collected by laser capture microscopy using a Veritas microdissection instrument (Arcturus, Life Technologies). Adjacent decidual cells were severed with the laser to prevent maternal contamination. Embryonic DNA was extracted using a QIAamp DNA micro kit from Qiagen, and the embryos were genotyped by PCR as described above.

Southern and Western blotting. Genomic DNA samples from either embryonic stem (ES) cells or tissues from TAF7-targeted or TAF7$^{+/-}$ mice were digested to completion using 120 U of NheI or NsiI. Digested samples were electrophoresed on 0.8% agarose gels in 1× Tris-borate-EDTA, transferred onto nitrocellulose membranes, and cross-linked using a UV cross-linker. The membranes were hybridized with the indicated probe labeled by nick translation and washed using high-stringency conditions. Soluble lysate fractions of 5×10^4 nuclei from green fluorescent protein-positive (GFP$^+$) MEFs and either uninfected TAF7$^{f/f}$ MEFs or TAF7$^{+/+}$ MEFs were analyzed by Western blotting with TAF7 antibody (Abcam, catalog no. 57494). The TFIID composition in MEFs was assayed either by direct Western blotting of soluble lysate from 2×10^6 nuclei or by TFIID immunoprecipitation performed on nuclear lysates from 3×10^6 MEFs with 2 μg of either TBP (Millipore), TAF4 (Santa Cruz), or TAF3 (kindly provided by Lazlo Tora). The TFIID components were separated by using a 4 to 20% gradient SDS-PAGE gel, and the following antibodies were used for Western blotting: TAF1 (Rockland, catalog no. 600-401-995), TAF2 (Novus Biologicals, NBP1-21371), TAF4 (SC-136093), TAF5 (SC-109058), TAF3, TAF6, TAF10 (kindly provided by Lazlo Tora), TAF12 (Proteintech, catalog no. 12353-1-AP), and TBP (Millipore, monoclonal antibody 3658). The composition of the TFIID complex in thymocytes or T cells was also assayed by direct Western blotting of 2×10^6 cell total extracts and using the antibodies described above.

Viral production and MEF infection. The MSCV-HA-TAF7-NGFR vector coding for both HA-TAF7 and NGFR proteins was generated by first inserting an oligonucleotide containing the hemagglutinin (HA) sequence in the BglII and EcoRI restriction sites of the MSCV-IRES-NGFR vector, kindly provided by W. Pear. The TAF7 sequence deleted of its stop codon was then introduced 5′ of the HA sequence at the BglII site. Either the MSCV-Cre-GFP vector encoding both the Cre recombinase and the GFP protein or the MSCV-HA-TAF7-NGFR was transfected in ecotropic PlatE cells (Cell Biolabs) using Fugene reagent (Roche), and the supernatant was collected 36 and 72 h posttransfection.TAF7$^{f/f}$ or wild-type (Wt) MEFs were transduced with either the murine stem cell virus (MSCV)-Cre-GFP retrovirus or the MSCV-HA-TAF7-NGFR retrovirus or both in the presence of Polybrene, and the cells were cultured in Dulbecco modified Eagle medium (DMEM) and 10% fetal calf serum (FCS) after infection. In the TAF7$^{f/f}$ or Wt MEFs infected by MSCV-Cre-GFP, the deletion of TAF7 was assayed by PCR by using Hot Start TaKaRa polymerase, and the growth of the cells was analyzed by flow cytometry. TAF7$^{f/f}$ MEFs infected by both MSCV-Cre-GFP and MSCV-HA-TAF-NGFR were purified by fluorescence-activated cell sorting (FACS) at 48 h postinfection (p.i.) based on the expression of GFP (green) and NGFR at the surface and established in culture. At 7 days p.i., the cells were counted and diluted for cloning. After expansion of the clones, the expression of both endogenous TAF7 and HA-TAF7 was tested, and the growth was analyzed.

PI staining. Cells were collected, fixed overnight in 70% ethanol, washed twice in phosphate-buffered saline (PBS), incubated in PBS 0.25% Triton X-100 for 15mn, washed again, resuspended in PBS supplemented with 1% bovine serum albumin, 10 μg of propidium iodide (PI), and 0.1 mg of RNase A, and then analyzed by flow cytometry (FACS).

Synchronization of cells. A total of 5×10^5 cells were sequentially cultured for 12 h in DMEM supplemented with 10% FCS and 2 mM thymidine (DMEM10/thymidine), for 16 h in medium without thymidine, and then for another 18 h in DMEM10/thymidine. Once the thymi-

dine removed, the cells were grown for 12 h and analyzed by FACS after PI staining.

Senescence assay. At 48 h after infection, GFP^+ cells were purified by flow cytometry, grown in DMEM–10% FCS, and analyzed at 8 days p.i. using a cellular senescence assay kit from Cell Biolabs.

Nuclear run-on assays. Nuclear run-on assays were performed according to standard procedures (5). Briefly, 2.5×10^5 to 5×10^5 nuclei in 25 mM HEPES (pH 7.5), 2.5 mM $MgCl_2$, 75 mM KCl, and 2.5 mM dithiothreitol were allowed to transcribe *in vitro* for 30 min at room temperature in the presence of [α-^{32}P]UTP (50 μCi), nonradioactive UTP (0.4 μM), and ATP/CTP/GTP (0.35 mM) with or without α-amanitin (50 μg/ml) (31). The radiolabeled RNAs were trichloroacetic acid precipitated twice for purification and counted.

***In vivo* run-on.** A total of 1.5×10^5 cells were grown on coverslips, incubated for 15 min in DMEM containing 2 mM 5-fluorouridine (Sigma, catalog no. F5130), fixed for 5 min with 4% paraformaldehyde in PBS, immunostained with rat anti-bromodeoxyuridine (anti-BrdU) antibody (AbD Serotec, catalog no. MCA2060T), and visualized using an Alexa Fluor 568-conjugated anti-rat antibody (Invitrogen, catalog no. A11077). To inhibit RNA Pol II elongation, the cells were cultured in the presence of α-amanitin at 50 μg/ml for 4 h prior to 5-fluorouridine incorporation. To provide an immunostaining control, a few coverslips with cells were treated after fixation with 50 μg of RNase A/ml to eliminate RNA during the immunostaining.

Expression profiling of MEF RNA. Both $TAF7^{f/f}$ and $TAF7^{+/+}$ MEF lines were infected by MSCV Cre-GFP retroviruses, and the infected cells (GFP^+) were isolated by FACS at 24, 48, and 72 h p.i. Uninfected cells from each line were harvested at the same time, collected by FACS, and processed simultaneously to be used as controls. The experiments were performed in triplicate. All RNAs were extracted by using shredders and an Qiagen RNeasy minikit, and their quality was assayed before they were used for hybridization. The total RNA from each of the triplicates was hybridized on the Affymetrix exon array. All exon array data were analyzed with Affymetrix expression console software (v1.1). The Robust Multiarray Analysis (RMA) algorithm was used for gene intensity analysis. Only genes in the "core" set, which represents RefSeq and full-length GenBank mRNAs, were included in the analysis. The three biological replicates are highly consistent as little variance was observed across triplicates (see Fig. 6C). For each MEF cell line ($TAF7^{f/f}$ and $TAF7^{+/+}$), we first identified genes that were up- or downregulated after infection by comparing the expression of infected cells to the uninfected cell line. For each pair of infected and uninfected samples, a list of significantly differentially expressed genes was selected with an absolute fold change greater than 1.414 (corresponding to the $\log_2$ scale at 0.5) and a *P* value (Student *t* test) of <0.05. Then, each $TAF7^{f/f}$ MEF cell line was paired to a $TAF7^{+/+}$ MEF cell line based on its RNA content, its growth curve, and the similarity of its overall expression profile. Any differentially expressed genes observed in the $TAF7^{+/+}$ MEF cell line as a result of transduction were removed from the analysis since they were caused by factors unrelated to the loss of TAF7 (such as genetic variations or cell growth- or infection-induced genes). A Gene Set Enrichment Analysis (GSEA) was performed for each gene list with Gene Ontology (GO) annotation and Kyoto Encyclopedia of Genes and Genomes (KEGG) annotation. Significant pathways were selected when the *P* value of a hypergeometric test was <0.05. The accession number for these data is GSE34793.

Purification of DN thymocytes and lymph node CD4 and CD8 T cells. For Western blotting, CD4, CD8 double negative (DN) thymocytes were purified according to the protocol for magnetic cell sorting (MACS) from Miltenyi Biotec. Totals of 6×10^7 thymocytes from either C57BL/6 or $TAF7^{f/+}$ LCK-Cre ($TAF7^{+/-}$) mice and 7×10^6 thymocytes from $TAF7^{f/-}$ LCK-Cre ($TAF7^{-/-}$) mice were incubated with a cocktail of MACS Pan T cells and CD4 and CD8 microbeads (Miltenyi Biotec, Inc.). DN thymocytes, depleted of all other thymocytes subpopulations, were recovered by passage through an LS magnetic separation column. For quantitative PCR and stimulation experiments, DN thymocytes were purified as described above, CD4 SP thymocytes were incubated with a cocktail of MACS CD8 microbeads (Miltenyi Biotec) and recovered with the DN thymocytes by passage through an LS magnetic separation column. Lymph node and spleen lymphocytes were incubated with a cocktail of MACS Pan T cell and either CD4 or CD8 microbeads, followed by passage through a LS magnetic separation column, to recover CD8 and CD4 T lymphocytes, respectively. Final isolation of the different populations of thymocytes and peripheral T cells was accomplished using flow cytometry based on cell surface expression as follows: DN, no T-cell receptor β (TCRβ), CD4, or CD8 expression; DP, low TCRβ, CD4, and CD8 expression; SP, high TCRβ, CD4, and CD8 expression; and naive and memory CD4T lymphocytes, high TCRβ expression and CD4 expression and, respectively, low or high CD44 expression.

Quantitative PCR. DNA from purified thymocytes or lymphocytes was prepared by using a Qiagen QIAamp DNA minikit, and quantitative PCR was performed using the SYBR green PCR Master mix from Applied Biosystems and the TAF7 and Slc25a2 oligonucleotide sets.

BrdU incorporation. Mice were injected in the peritoneal cavity with 1 mg of BrdU twice, at 2 and 4 h before the thymuses were harvested. The cells were fixed and treated according to the procedure described in the BrdU flow kit (BD Pharmingen). DN thymocytes were identified by the absence of staining with a cocktail of antibodies recognizing surface proteins expressed on lineage-committed cells (TCRβ, CD4, CD8, B220, NK1-1, MACI, and GR-1) and CD44 and CD25 antibodies and assessed for BrdU incorporation by flow cytometry.

TCRβ intracellular staining. DN thymocytes were identified as described above and fixed using Cytofix/Cytoperm solution (BD Pharmingen), internally stained with an anti-TCRβ antibody, and the DN analyzed by flow cytometry.

Stimulation of T cells. Lymph node lymphocytes were incubated with a cocktail of MACS Pan T cell and CD8 microbeads and the CD4 lymphocytes recovered by passage through an LS magnetic separation column. A total of 10^5 CD4 T cells were plated on plates previously coated with either 10 μg of NA/LE anti-CD3e antibody or 10 μg of NA/LE anti-CD3e and 1 μg of NA/LE anti-CD28 antibody. The cells were grown for 72 h in RPMI 1640 medium supplemented with 10% FCS and 2-mercaptoethanol with or without interleukin-2 (IL-2; 200 U/ml); their ability to proliferate was assayed by either counting the cells or adding 1 μCi of [^{3}H]thymidine for 8 h in the culture medium and counting the radioactive thymidine incorporation.

Microarrays on CD4 naive T cell RNAs. CD4 T cells were isolated as described above from 5×10^8 spleen lymphocytes. RNAs were extracted using Qiagen shredders and the RNeasy minikit from Qiagen, and their quality was assayed before using them for hybridization. RNA was processed and hybridized on a GeneChip Human Gene 1.0 ST array (Affymetrix, Santa Clara, CA) according to the manufacturer's protocol. The intensity data from the Affymetrix GeneChips were normalized and annotated with Affymetrix expression console software by using RMA-Sketch workflow. Cutoffs of 1.5- and 2-fold changes (corresponding to $\log_2$ scales of 0.585 and 1, respectively) were used to identify the differentially expressed genes in $TAF7^{-/-}$ and $TAF7^{+/-}$ T cells. For GSEA, the GSEA method from Broad (http://www.broad.mit.edu/gsea/) was applied to investigate the enrichment of PID_TCR_SIGNALING and TAF_GENE_SET. The PID_TCR_SIGNALING gene set was constructed by using all of the genes involved in BIOCARTA_TCR_PATHWAY, REACTOME_TCR_SIGNALING, KEGG_T_CELL_RECEPTOR_SIGNALING_PATHWAY, and NATURE_NCI_TCR_SIGNALING_IN_NAIVE_CD4+_T_CELLS. The TAF_gene_set was constructed by including all TAF genes and the TBP gene. In the case of multiple probe sets representing the same gene, the median of intensity values were taken. The accession number for these data is GSE34795.

RESULTS

TAF7 gene disruption results in early embryonic lethality. To examine TAF7 gene function *in vivo*, we generated a floxed allele

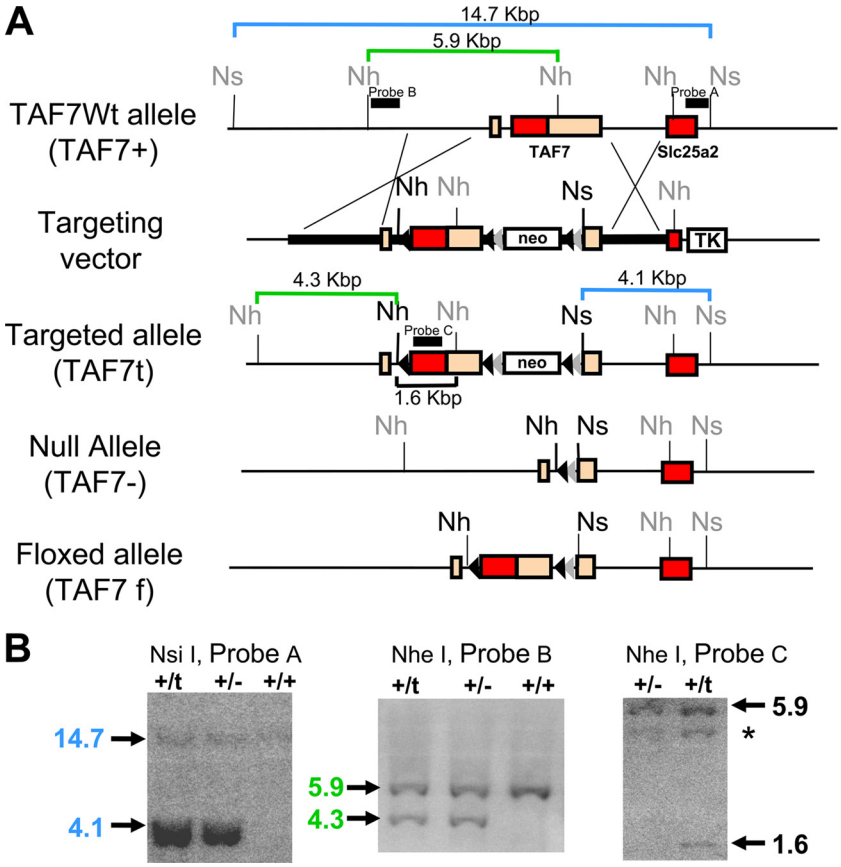

FIG 1 Strategy for the generation of the conditional TAF7 knockout. (A) Schematic diagrams of the TAF7 wild-type (TAF7Wt), targeted (TAF7t), null (TAF7−), and floxed (TAF7f) alleles. The wild-type TAF7 gene is composed of two exons (rectangles) and one intron (thin black lines between exons). The first exon is a noncoding exon consisting of 5′ untranslated region (5′UTR) sequences (orange rectangle). The second exon contains all of the coding sequences (red rectangle) necessary for the expression of the TAF7 protein and a long noncoding 3′UTR (orange rectangle). A targeting construct was generated by homologous recombination by inserting a loxP site (black triangle) within the first intron of the TAF7 gene and a frt-loxP-neo-frt-loxP cassette in the noncoding sequence of the second exon. The targeted (TAF7t) allele was then generated by homologous recombination in ES cells. The TAF7-null allele (TAF7−) was generated by β-actin-Cre-mediated deletion of the floxed region, including the *neo* cassette and the TAF7 coding region; the TAF7 floxed allele (TAF7f) was generated by Flpe-mediated deletion of the *neo* cassette. Black triangles, loxP sites; gray triangles, frt sites; Slc25a2, neighboring downstream gene. (B) Genotyping of the TAF7Wt, TAF7t, and TAF7− alleles. The replacement of the Wt allele by the targeted allele and further the deletion of TAF7 were tested as described: spleen genomic DNA from either $TAF7^{+/t}$, $TAF7^{+/-}$, or Wt mice were digested either by NheI or NsiI and Southern blot hybridized with corresponding probes. The positions of the relevant restriction sites (Nh, NheI; Ns, NsiI), the probes used for Southern blotting, and the sizes of the expected fragments are indicated. *, Nonspecific band inconsistently revealed in Wt, $TAF7^{+/t}$, and $TAF7^{+/-}$ mouse DNA.

of the mouse TAF7 gene, with loxP sites flanking its entire coding region (Fig. 1A). Germ line deletion was accomplished by breeding with β-actin-Cre mice. Heterozygous $TAF7^{+/-}$ mice and wild-type (Wt) mice were identified based on their distinct restriction fragment patterns (Fig. 1B). Heterozygous $TAF7^{+/-}$ mice, in which only one allele is deleted, were phenotypically indistinguishable from their $TAF7^{+/+}$ littermates and were normal, healthy, and fertile (data not shown). Furthermore, in crosses between $TAF7^{+/-}$ heterozygotes and $TAF7^{+/+}$ Wt mice, the ratio of $TAF7^{+/-}$ to $TAF7^{+/+}$ animals was not significantly different from the expected 1:1 ratio, which is consistent with the lack of phenotype in heterozygous $TAF7^{+/-}$ mice (data not shown). These results indicate that heterozygous $TAF7^{+/-}$ mice are not haploinsufficient for TAF7. In striking contrast, intercrosses of $TAF7^{+/-}$ mice generated no homozygous $TAF7^{-/-}$ mice among 139 pups tested (Table 1). Thus, homozygous deletion of TAF7 was embryonic lethal, demonstrating that TAF7 is essential for normal mouse development.

To establish the stage at which development of $TAF7^{-/-}$ embryos are arrested, we harvested embryos from $TAF7^{+/-}$ intercrosses at different times of gestation and genotyped them. At 11.5 dpc (when organogenesis begins), no $TAF7^{-/-}$ embryos were detected. Furthermore, no $TAF7^{-/-}$ embryos were detected among the 52 examined at 8.5 dpc (four-somite stage, when embryonic structure is evident) (Table 2). Thus, TAF7 is required prior to

TABLE 1 Homozygous TAF7 deletion results in embryonic lethality: no $TAF7^{-/-}$ offspring were recovered from $TAF7^{+/-}$ intercrosses[a]

Offspring genotype	No. of offspring (n = 139)
$TAF7^{+/+}$**	53
$TAF7^{+/-}$	86
$TAF7^{-/-}$*	0

[a] A total of 139 pups from intercrosses between $TAF7^{+/-}$ mice were tested for the presence of the TAF7 Wt allele. Significance was calculated as "observed" relative to "expected" by chi-squared analysis: *, $P < 0.0001$; and **, $P > 0.28$.

TABLE 2 Homozygous TAF7 deletion results in embryonic lethality: no TAF7$^{-/-}$ embryos were detected at 5.5 dpc or later[a]

Embryo age (dpc)	No. of decidua	No. of empty decidua	No. of embryos		
			TAF7$^{+/+}$	TAF7$^{+/-}$	TAF7$^{-/-}$
>11.5	39	13	11	15	0*
8.5	52	20	14	18	0**
5.5	32	16	7	9	0***

[a] Embryos from TAF7$^{+/-}$ intercrosses were harvested at different times of gestation and genotyped. The significance was calculated as "observed" relative to "expected" by chi-squared analysis: *, $P < 0.005$; **, $P < 0.0017$; and ***, $P < 0.041$.

these two developmental stages. Interestingly, in the analysis of the decidua at 8.5 dpc, empty decidua (or decidua containing only a few membranes) occurred at a frequency consistent with that expected for TAF7$^{-/-}$ embryos, suggesting that TAF7-deficient embryos could survive until implantation at 4.5 dpc.

To determine whether TAF7$^{-/-}$ embryos can implant and expand, we examined uteri obtained from 5.5-dpc pregnant females. In a heterozygous cross, both decidua with normally developing embryos (Fig. 2A, left) and empty decidua (Fig. 2A, right) were observed. Of the 32 sectioned decidua, 16 embryos could be harvested by laser capture microscopy. No TAF7$^{-/-}$ embryos were identified (Table 2), suggesting that TAF7$^{-/-}$ embryos were able to elicit a decidual response but were not able to either implant or expand.

To further define the stage at which development of TAF7$^{-/-}$ embryos is arrested, we collected 3.5-dpc blastocysts from TAF7$^{+/-}$ intercrosses, maintained them in culture for 2 days to eliminate any maternal contamination, and then genotyped them. Three of the sixteen blastocysts collected were negative for both TAF7 alleles (Fig. 2B), a finding consistent with the expected frequency of 25%. Of the 16 blastocysts collected, 5 hatched during the 2-day culture (data not shown). Among them, one was a TAF7$^{-/-}$ blastocyst, indicating that TAF7$^{-/-}$ embryos are capable of developing at least until hatching at ~4.5 dpc. (TAF7L, the paralog of TAF7 in testis [6], does not substitute for TAF7 since it is not expressed in blastocysts [data not shown].) These studies demonstrate that TAF7 gene deletion leads to embryonic lethality between 3.5 and 5.5 dpc.

TAF7 is required for the proliferation and survival of immortalized MEFs. Between 5.5 and 8.5 dpc, embryos undergo a massive proliferative expansion (19). The fact that no TAF7$^{-/-}$ embryo could be recovered after 5.5 dpc suggested that TAF7 is required for cellular proliferation and/or survival. To further examine the role of TAF7 in cell growth and/or survival, we investigated the requirement for TAF7 in MEF cell lines. Two MEF cell lines (the TAF7 f/f-1 and f/f-2 cell lines) were generated from 13.5-dpc embryos homozygous for the floxed TAF7 allele (TAF7$^{f/f}$) (Fig. 1A). The TAF7$^{f/f}$ MEF cell lines expressed TAF7 but not the homolog TAF7L (data not shown). In parallel, two control TAF7$^{+/+}$ MEF cell lines (Wt) were established in parallel from 13.5 dpc wild-type embryos.

TAF7 gene deletion in TAF7$^{f/f}$ MEFs was accomplished by infection with MSCV-Cre-GFP retroviruses. GFP^{+} infected cells were purified by flow cytometry at 24 and 48 h p.i.; the extent of TAF7 gene deletion was monitored as a function of time after infection. By 24 h p.i. of the TAF7$^{f/f}$ MEFs, the novel fragment generated upon TAF7 deletion (Fig. 3A, upper panel, null fragment) was robustly evident, and almost no native TAF7 genomic DNA remained (Fig. 3A, upper panel, TAF7f fragment, and lower panel, Flox fragment). Accordingly, TAF7 protein expression was markedly depleted by 48 h p.i (data not shown); by 72 to 120 h p.i., no detectable TAF7 protein remained (Fig. 3B and data not shown).

TAF7 is a component of the highly structured TFIID complex and interacts with TBP and TAF1 in a submodule of TFIID (8). As we have shown previously, TAF7 binds to and inhibits the essential activity of the acetyltransferase domain of TAF1 (13). Therefore, we next sought to determine whether TAF7 depletion affects the expression of TAF1 or any of the other TAFs, either in the total nuclear extract or in the TFIID complex. As detected by Western blotting, all of the TAFs tested were present in total nuclear extracts of TAF7-null MEFs (Fig. 4A, center) and, with the exception of TAF7, at relative abundances not significantly different from the uninfected control (Fig. 4A, center, and B). The composition of TFIID also was not altered as a result of TAF7 depletion. The patterns of TAFs coimmunoprecipitated in TFIID by either anti-TBP or anti-TAF4 were indistinguishable between TAF7$^{-/-}$ and Wt MEFs, with the exception of TAF7 (Fig. 4A, left panel). Thus, the loss of TAF7 does not result in an overall destabilization of the existing TFIID complex.

Surprisingly, TFIIDs from both TAF7$^{-/-}$ and Wt MEFs were devoid of TAF3, although TAF3 was abundant in the total nuclear extracts (Fig. 4A). TAF3 was not coimmunoprecipitated with either anti-TBP or anti-TAF4 under conditions that identified the remaining TAFs (Fig. 4A, left). Conversely, anti-TAF3 immunoprecipitated TAF3, but not TBP, from nuclear extracts (Fig. 4A, right). The absence of TAF3 in these MEFs contrasts with a report by Choukrallah et al. (7) in which TAF3 was recovered in TFIID. These differences in TFIID composition may reflect either the origin of the MEFs or the methods used to establish the MEFs: in the previous report, the MEFs were immortalized with simian virus 40 T antigen, whereas in the present study the MEFs were immortalized spontaneously.

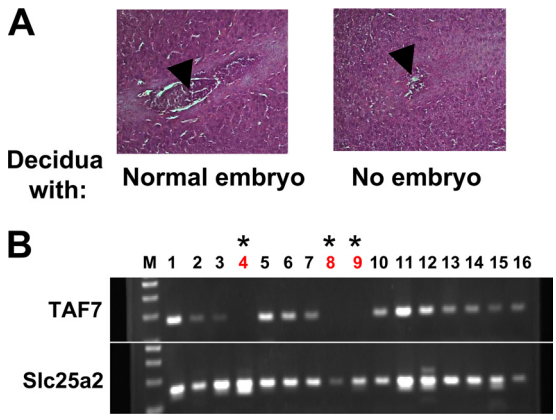

FIG 2 TAF7 is required early in development. (A) TAF7$^{-/-}$ embryos do not survive beyond 5.5 dpc. Hematoxylin-and-eosin-stained sections of uteri from 5.5-dpc TAF7$^{+/-}$ heterozygous intercrosses. Two types of decidua were observed: decidua with normally developing +/+ or +/− embryos (left side, which were genotyped as +/+ or +/−) and empty decidua with no embryonic structure (right side, no genotyping possible). (B) TAF7$^{-/-}$ embryos derived from TAF7$^{+/-}$ intercrosses develop until 3.5 dpc. Blastocysts were recovered at 3.5 dpc and genotyped by PCR using different sets of oligonucleotides to detect TAF7 (upper panel) and *Slc25a2* genes (lower panel). *, TAF7$^{-/-}$ blastocysts.

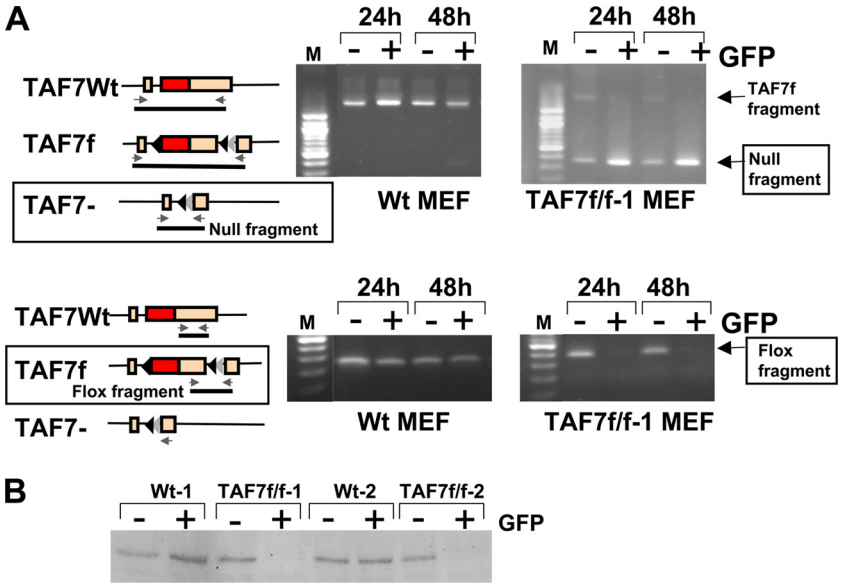

FIG 3 TAF7 deletion in the TAF7 f/f-1 MEF line is complete by 48 h p.i. (A) TAF7 excision is complete by 48 h. Either TAF7 f/f-1 or TAF7 Wt MEFs exposed to MSCV-Cre-GFP were purified by flow cytometry 24 and 48 h p.i. GFP^+ and GFP^- cells were purified and genotyped by PCR for the presence of the TAF7-null allele (A, top) and the disappearance of the floxed TAF7 gene (A, bottom). On the left, are shown the oligonucleotide sets used for the genotyping (small arrows) and the expected fragments (thick black lines): TAF7 deletion generates a specific fragment (null fragment) and the loss of TAF7 sequences (Flox fragment). The presence of the null fragment (A, top) in the GFP^- purified population indicates that a fraction of the GFP^- cells were infected but did not express detectable GFP. M, molecular weight marker. (B) TAF7 protein depletion is complete in the infected MEF cells. TAF7 f/f-1 MEFs either infected or not infected with MSCV-Cre-GFP were purified by flow cytometry at 48 h p.i., cultured for three more days, and then lysed. Their soluble fractions were analyzed by Western blotting with a TAF7 antibody.

To evaluate the functional requirement for TAF7 in the MEF cell lines, we monitored the growth and survival of TAF7-null and wild-type MEF cells. $TAF7^{f/f}$ and TAF7 Wt MEFs were transduced with the MSCV Cre-GFP retrovirus under conditions in which virtually all of the cells are transduced, and their growth was monitored for 5 days p.i. As shown in Fig. 5A, uninfected $TAF7^{f/f}$ or infected TAF7Wt MEF lines continued to grow throughout the 5-day culture period. In contrast, expansion of the TAF7-null cell lines was dramatically impaired at 3 days p.i.; significant cell loss occurred by 5 days p.i. By day 8 p.i., only a very few cells survived. Of the remaining cells, nearly half (46%) stained positive with trypan blue (Fig. 5A, f/f-1/Cre+, and data not shown). Similar growth kinetics were obtained if GFP^+ cells were purified by flow cytometry at 24 h p.i., plated, and monitored relative to control cells (Fig. 5A, f/f-2/Cre+). The cell loss is a direct result of TAF7 depletion, since the transduction of Cre-infected $TAF7^{f/f}$ MEFs with exogenous TAF7 rescues cell viability and growth at a rate comparable to that of Wt MEFs (Fig. 5B). Thus, embryonic fibroblast cells devoid of TAF7 stop proliferating, and most fail to survive.

Loss of TAF7 did not acutely arrest cells at any stage of the cell cycle, as assessed by PI staining. However, there was a modest enrichment of cells at G_2/M after the infection of unsynchronized cells or after the release from synchronization of infected cells (Table 3). Thus, TAF7 appears to be necessary throughout cell cycle, a finding consistent with the broader role for TAF7 in transcription initiation beyond its presence in TFIID (13).

We next sought to determine whether TAF7 gene deletion initiated a specific death pathway: apoptosis, autophagy, or senescence. No significant accumulation of apoptotic cells (as measured by annexin V staining or chromatin condensation) was detected at any time after infection of either $TAF7^{f/f}$ MEFs or control infected TAF7 Wt MEFs (data not shown). We also saw no evidence that TAF7 depletion induced autophagy, as indicated by the levels of LC3b II and SQSTM1 proteins (19, 27) in $TAF7^{f/f}$ infected MEFs relative to control TAF7 Wt infected MEFs (data not shown). Of the few TAF7-null MEFs remaining at 8 dpi, a significant number expressed senescence-associated β-galactosidase, a finding indicative of a senescence-like phenotype (Table 4). However, we did not detect the expression of other senescence markers (9), such as P21, P16, and SHARP2 in the TAF7-null $TAF7^{f/f}$ MEFs, which may reflect the inability to transcribe these genes when TAF7 levels are depleted or markedly reduced (data not shown). These observations suggest that neither apoptosis nor autophagy is a major pathway leading to cell loss in TAF7-deficient cells; the few $TAF7^{-/-}$ cells that do survive exhibit a senescence-like phenotype. The mechanism of cell death remains to be determined.

TAF7 deletion affects global transcription in MEFs. We previously provided evidence that TAF7 is a regulator of the early steps of transcription initiation, that it affects the expression of ca. 65% of transcripts in 293 kidney cells, and that, of those, some are TAF1 dependent, while others are TAF1 independent (3). Therefore, we next sought to determine whether TAF7 is dispensable for a subset of embryonic fibroblast genes or whether it is required globally. A gross estimate of the extent of total *de novo* transcription in infected $TAF7^{f/f}$ MEFs and control TAF7 Wt MEF cell lines was made in two independent ways. First, we measured [^{32}P]UTP incorporation in nuclear run-on assays performed at 4 days p.i. As shown in Fig. 6A, *de novo* RNA synthesis is significantly impaired by the deletion of TAF7. The RNA Pol II inhibitor, α-amanitin, does not appreciably reduce synthesis beyond that achieved by

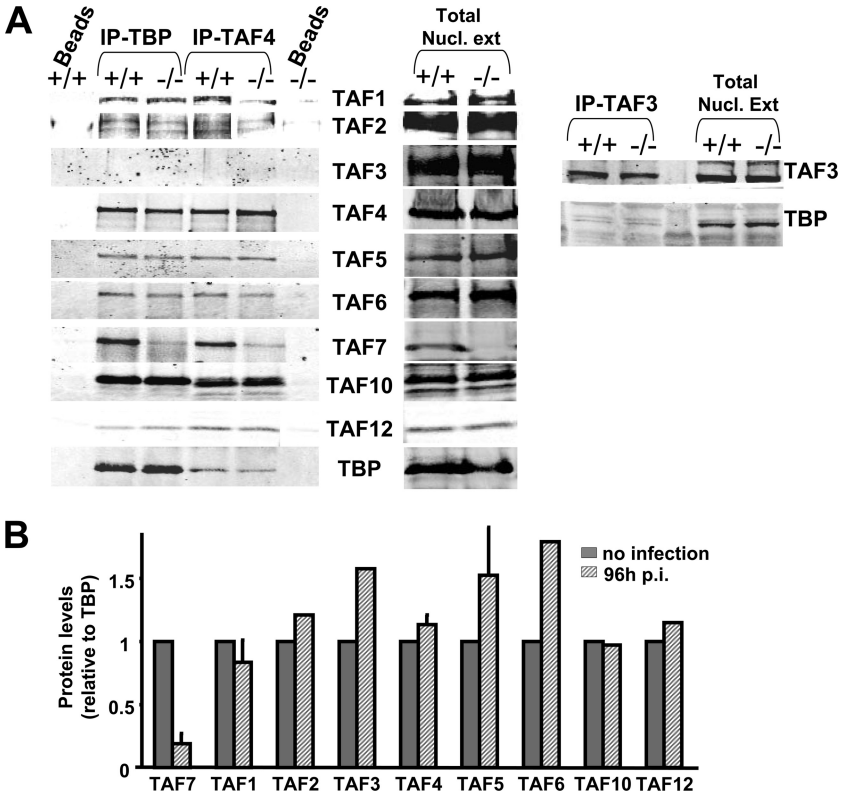

FIG 4 TAF7 deletion does not affect the level of other TFIID components and does not prevent TFIID assembly. (A) TAF7 deletion does not prevent TFIID assembly. At 4 days p.i., the different TFIID components in GFP$^+$ or noninfected TAF7$^{f/f}$ MEFs were analyzed by Western blotting, as indicated either directly from soluble nuclear extract (center) or after immunoprecipitation using either anti-TBP (IP-TBP) or anti-TAF4 (IP-TAF4) (left) or anti-TAF3 (IP-TAF3) (right) antibodies. Beads correspond to a control immunoprecipitation with no antibody on the beads. (B) TAF7 depletion does not significantly affect the level of other TAFs. The relative abundances of different TAFs in nuclear extracts shown in panel A were determined by densitometry and normalized relative to the levels of TBP in infected versus uninfected MEFs. (Since TAF7 depletion affects MEF transcription globally, it was not possible to correct based on an independent loading control.)

TAF7 deletion alone, suggesting that TAF7 deficiency leads to a global reduction in transcription in embryonic fibroblasts. The remaining α-amanitin-resistant, and presumably TAF7-independent, synthesis represents Pol I and Pol III ribosomal and small RNA transcription, which is largely insensitive to the inhibitor under the conditions used (31).

To further examine the effect of TAF7 depletion on transcription, TAF7$^{-/-}$ and f/f MEFs were pulsed with 5-fluorouridine at 5 and 7 days p.i. The extent of incorporation into RNA after a 15-min pulse was determined by fluorescence microscopy. As shown in Fig. 6B (upper panels), after TAF7 depletion *de novo* RNA synthesis in the nucleoplasm is abrogated. The extent of transcriptional inhibition parallels that achieved by α-amanitin treatment (Fig. 6B, lower panels). Taken together, our findings indicate that TAF7 depletion results in a global loss of *de novo* transcription.

Although global inhibition of transcription was observed late in infection, when no TAF7 remained, we considered the possibility that TAF7 depletion initially spares a subset of transcripts, as observed in the differentiated 293 kidney line. To this end, we analyzed the RNA expression profiles of the two independent TAF7$^{f/f}$ MEF cell lines at 24, 48, and 72 h p.i. As determined by expression analysis, TAF7 levels were reduced by >100-fold by 24 h in f/f-1 MEFs and by 48 h in f/f-2 MEFs, relative to their uninfected controls. Surprisingly, the basal patterns of gene expression, prior to TAF7 deletion, differed markedly between the two TAF7$^{f/f}$ cell lines, suggesting that they derive from distinct developmental lineages (Fig. 6C, compare the profiles of the two uninfected lines; G. Wu et al., unpublished data). Importantly, TAF7 deletion did not selectively block expression of a subset of transcripts at any time point assayed in either of the two lines. Rather, TAF7 deletion led to a global decrease in all transcripts, consistent with the observed general cessation of *de novo* Pol II RNA synthesis. Although a small number of transcripts in both TAF7$^{f/f}$ MEF lines did display net changes at the different time points that were validated by reverse transcription-PCR (data not shown), none was observed consistently, either at different time points in a single TAF7$^{f/f}$ line or between the two lines. We speculate that these transcripts may have exceptionally high or low RNA turnover rates. We conclude that in contrast to 293 kidney cells, TAF7 deletion in embryonic fibroblast lines leads to a global arrest of transcription, resulting in a cell cycle-independent block in proliferation.

TAF7 is required during the early steps in thymic development. The disparity between the global effects of TAF7 depletion on gene expression in embryonic fibroblasts and the restricted effects in differentiated 293 kidney cells (3) led us to consider the possibility that dependence on TAF7 decreases during differentiation. To this end, we examined the role of TAF7 in thymocyte development, an *in vivo* differentiation system which has been extensively characterized (for review, see reference 4). The stages

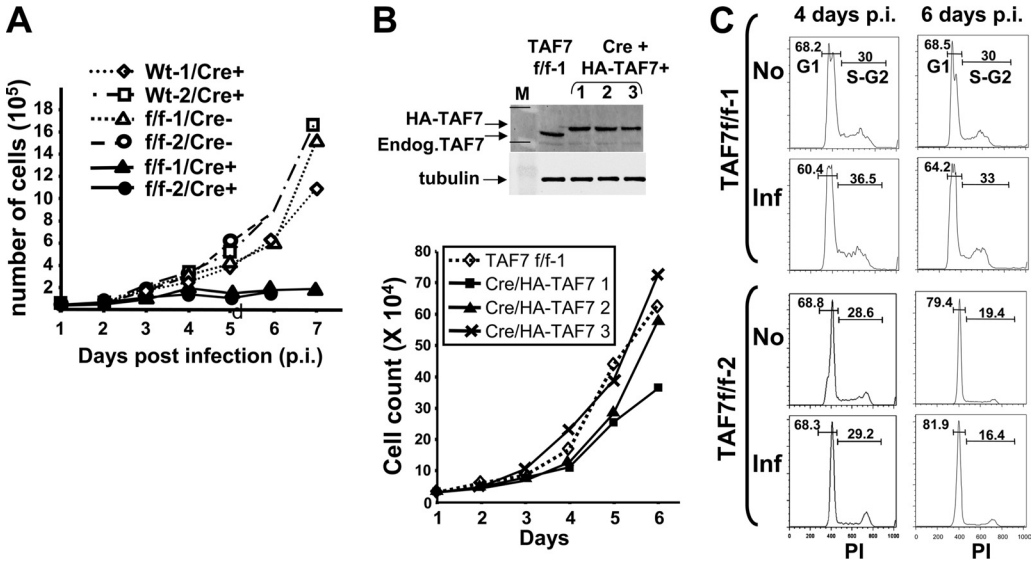

FIG 5 TAF7 is necessary for proliferation and/or survival of MEFs. (A) MEFs deleted of TAF7 cease proliferating. GFP$^+$ cells from either TAF7$^{f/f}$ (f/f-1 and f/f-2) or TAF7$^{+/+}$ (Wt-1 and Wt-2) MEF lines infected with MSCV-Cre-GFP (Cre+) were plated and counted at the times indicated. MEF f/f-2 cells were purified by flow cytometry prior to plating. The growth of noninfected TAF7$^{f/f}$ cells (Cre−) was assessed in parallel. (B) Exogenous TAF7 restores cell proliferation and survival in TAF7-depleted MEFs. The expression of both endogenous TAF7 (endog. TAF7) and heterologous HA-TAF7 (HA-TAF7) was tested by Western blotting in three TAF7$^{f/f}$ MEF clones infected by both MSCV-Cre-GFP and MSCV-HA-TAF7-NGFR (top). The relative growth capacity of these three clones was compared to the original TAF7$^{f/f}$ MEFs (bottom). (C) MEFs depleted of TAF7 are not blocked at a specific stage of the cell cycle. The cell cycle distribution of TAF7$^{-/-}$ GFP$^+$ or noninfected TAF7$^{f/f}$ or TAF7$^{+/+}$ MEF cells was analyzed by PI staining at 4 and 6 days p.i.

of thymocyte differentiation are distinguished by the patterns of expression of two cell surface molecules CD4 and CD8 (Fig. 7A). The most immature precursors express neither CD4 nor CD8 (double-negative [DN] thymocytes). Upon rearrangement of the T-cell-receptor β gene (TCRβ), DN thymocytes undergo massive proliferation and begin to express both CD4 and CD8, thereby becoming double-positive (DP) thymocytes, which rearrange their TCRα genes. Those DP thymocytes expressing assembled surface TCRαβ with appropriate avidity for major histocompatibility complex (MHC) class II or class I molecules lose either CD8 or CD4 expression to become CD4 (CD4 SP) or CD8 (CD8 SP) single-positive thymocytes, respectively. Whereas the DN-to-DP transition is accompanied by a major proliferative burst, the DP-to-SP transition occurs without further cell division.

To examine the role of TAF7 in early thymic differentiation at the DN-to-DP transition, we generated heterozygous TAF7$^{f/-}$ LCK-Cre mice that express Cre driven by the proximal LCK promoter, which is active in early DN thymocytes, prior to the proliferative burst (Fig. 7A) (22). This results in TAF7 gene deletion prior to the DN-to-DP transition, allowing us to assess the requirement for TAF7 in both proliferation and subsequent differentiation. In the thymuses of the TAF7$^{f/-}$ LCK-Cre mice, the majority of the DN and DP thymocytes have the remaining TAF7 allele deleted compared to either Wt or TAF7$^{f/-}$ heterozygous mice, as determined by the levels of the TAF7 allele (Fig. 7B). TAF7 protein in the DN cells is also dramatically reduced relative to Wt and TAF7$^{+/-}$ mice, as assessed by Western blotting (inset to Fig. 7B).

The TAF7$^{f/-}$ LCK-Cre mice have very small thymi compared to the Wt (TAF7$^{+/+}$) or heterozygous TAF7$^{+/-}$ mice, reflecting a

TABLE 3 MEFs depleted of TAF7 are not blocked at a specific stage of the cell cycle[a]

Time (h)	Thymidine block	Distribution (%)					
		Uninfected cells			Infected cells		
		G_1 phase	S phase	G_2/M phase	G_1 phase	S phase	G_2/M phase
$R = 0$	No	64	20.8	11.9	51.6	15.2	24.3
	Yes	50.1	33.8	12.1	51	18.7	22
$R = 12$	No	57.6	20.3	18.5	50.9	14	27
	Yes	54.1	23	19.8	46.8	14.9	30.6

[a] Distribution of uninfected and GFP$^+$ infected TAF7$^{f/f}$ cells throughout cell cycle after release from double thymidine block and measurement by PI staining. $R = 0$, release from the second thymidine block; $R = 12$, 12 h after the release of the second thymidine block.

TABLE 4 TAF7$^{-/-}$ MEFs surviving until 8 days p.i. display a senescence-like phenotype[a]

Type	Cre	No. of cells		
		Total no. of cells	β-Gal$^+$ cells	βGal$^+$ cells/total cells (%)
Wt-1	–	200	0	0
	+	234	1	0
Wt-2	–	190	0	0
	+	162	6	4
f/f-1	–	114	0	0
	+	131	12	9
f/f-2	–	200	1	0
	+	153	73	48

[a] Either infected GFP$^+$ TAF7$^{f/f}$ (+) or uninfected TAF7$^{f/f}$ (–) MEFs were assayed for senescence-associated (SA) β-galactosidase (β-Gal) as described in Materials and Methods, and the numbers of cells expressing the SA β-galactosidase were determined at 8 days p.i. Either infected or uninfected Wt MEFs were assayed in parallel.

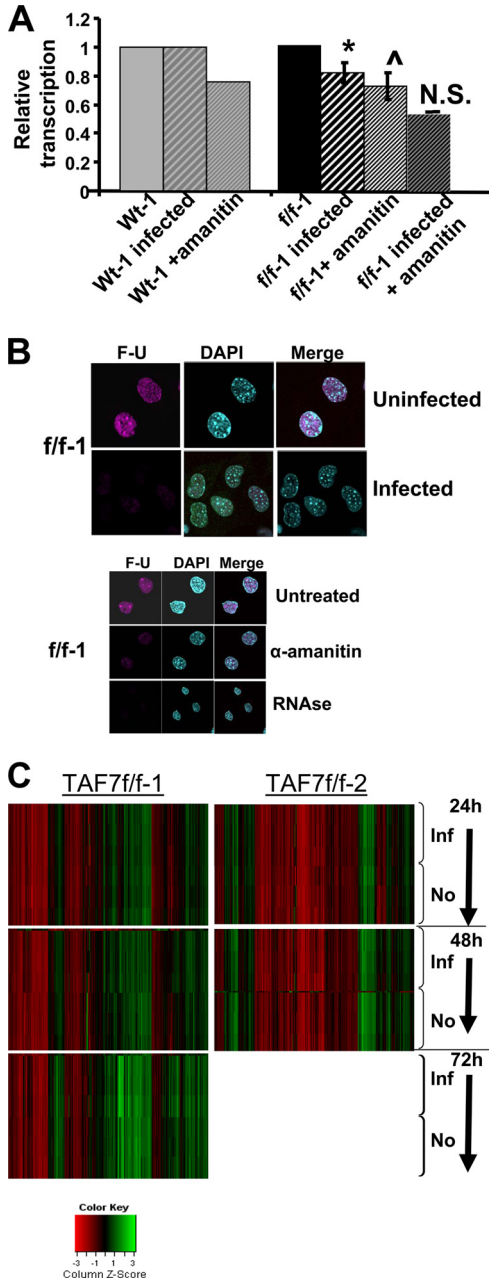

FIG 6 TAF7 depletion has a global effect on gene transcription. (A) TAF7 depletion has a global effect on gene transcription. *In vitro* RNA synthesis in nuclear run-ons of either GFP$^+$ cells from infected (Wt-1 infected) or noninfected (Wt-1) TAF7 Wt (left side) or infected (f/f-1 infected) or noninfected TAF7$^{f/f}$ (f/f-1) MEF cultures (right side) incubated in the presence or absence of 50 μg of α-amanitin/ml. *, significant differences between f/f-1 uninfected and f/f-1 infected samples; ^, significant difference between uninfected f/f-1 and f/f-1 plus α-amanitin samples; NS, nonsignificant difference between f/f-1-infected and f/f-1-infected + α-amanitin samples. (B) TAF7 depletion has a global effect on Pol II transcription. (Top) Either infected or noninfected TAF7 f/f-1 MEF cells were cultured in the presence of 2 mM 5-fluorouridine fixed and immunostained using an anti-BrDU antibody. Nuclei are revealed by a DAPI staining. (Bottom) Noninfected TAF7 f/f-1 MEF cells were either cultured for 5 h in the presence of α-amanitin before treatment with 5-fluorouridine or exposed to RNase after 5-fluorouridine treatment and fixation. The incorporation of 5-fluorouridine is detected as described above by staining with an anti-BrdU antibody. (C) Overall gene expression patterns do not differ in the presence or absence of TAF7 in TAF7$^{f/f}$ lines. TAF7 MEF lines were infected by MSCV Cre-GFP retroviruses, and the infected cells (GFP$^+$) were isolated by FACS as indicated. Cell death was sufficiently advanced in infected TAF7 f/f-2 cells that they could not be analyzed at 72 hrs p.i. Uninfected cells were harvested and processed in parallel. Total RNA from infected or noninfected TAF7$^{f/f}$ MEFs were analyzed on the Affymetrix exon array, and the top 5% most variable genes presented as shown. The experiment was performed in triplicate.

dramatic reduction in the total number of thymocytes (Fig. 7C). This decrease reflects a massive reduction in the number of DP thymocytes ($3.6 \times 10^6 \pm 0.7 \times 10^6$ in TAF7$^{-/-}$ mice versus $1.75 \times 10^8 \pm 0.35 \times 10^8$ in Wt mice) and of CD4 SP and CD8 SP cells ($7.0 \times 10^5 \pm 2.5 \times 10^5$ and $3.0 \times 10^5 \pm 2 \times 10^5$, respectively, in TAF7$^{-/-}$ mice versus $10.9 \times 10^6 \pm 1.9 \times 10^6$ and $2.4 \times 10^6 \pm 0.5 \times 10^6$ in Wt mice). In contrast, the absolute number of DN thymocytes in TAF7$^{f/-}$ LCK-Cre mice was not diminished relative to either Wt or TAF7$^{+/-}$ thymi (Fig. 7C) but, instead, was slightly increased compared to the Wt thymus ($8 \times 10^6 \pm 1 \times 10^6$ in TAF7$^{-/-}$ mice versus $5 \times 10^6 \pm 0.8 \times 10^6$ in Wt mice). Thus, TAF7 is required for the transition from DN to DP, coincident with the large burst of cellular proliferation. Consistent with the huge reduction in the double- and single-positive thymocyte populations, the number of mature CD4$^+$ (CD4T) and CD8$^+$ (CD8T) T cells in the spleen was also sharply reduced ($4 \times 10^6 \pm 1 \times 10^6$ and $2 \times 10^6 \pm 0.2 \times 10^6$, respectively, in TAF7$^{-/-}$ mice versus $13 \times 10^6 \pm 2.5 \times 10^6$ and $8 \times 10^6 \pm 2 \times 10^6$ in Wt mice). However, the ratio between the two populations was maintained in TAF7$^{-/-}$ mice relative to Wt mice (Fig. 7D). The few CD4 and CD8 T cells recovered from the spleen had Wt levels of the TAF7 allele, indicating that only thymocytes that escape deletion at the DN stage can differentiate to mature peripheral T cells (Fig. 7B).

TAF7-deficient DN thymocytes have a defect in proliferation. The small number of DP thymocytes observed in the TAF7$^{-/-}$ thymus could be due to a defect in either proliferation and/or signaling of the DN thymocytes or a survival defect in DP thymocytes. DN thymocytes go through four developmental stages (DN1 to DN4) that are distinguishable by their surface expression of CD44 and CD25 (Fig. 7E). While cells in the DN2 stage undergo modest proliferation, the major burst of proliferation occurs at the DN4 stage. Proximal LCK promoter activity is first detected at the DN2 stage, prior to TCRβ gene rearrangement. To determine whether DN thymocytes can proliferate in the absence of TAF7, we tested their ability to incorporate BrdU following TAF7 deletion. TAF7$^{f/-}$ LCK-Cre mice and control TAF7$^{f/+}$ LCK-Cre mice were injected with BrdU at 2 and 4 h prior to harvesting thymocytes. The incorporation of BrdU was assessed in the DN3 and DN4 thymocyte subpopulations by flow cytometric analysis (Fig. 7F) (the numbers of DN1 and DN2 were too small to assess). BrdU incorporation was markedly reduced in DN4, but not DN3, thymocytes from TAF7$^{f/-}$ LCK-Cre mice, relative to control thymocytes. Consistent with a defect in the TAF7$^{-/-}$DN4 thymocytes, TCRβ expression was markedly lower than in Wt DN4 thymocytes (Fig. 7G); expression was normal in the TAF7$^{-/-}$ DN3 cells. Thus, deletion of TAF7 results in a defect in the proliferation of DN4 thymocytes and an associated block in differentiation.

TAF7 is not required for the final steps in thymocyte development. The experiments described above suggest that TAF7 is important for the *in vivo* proliferation of DN thymocytes that leads to the generation of DP thymocytes. Since the total number

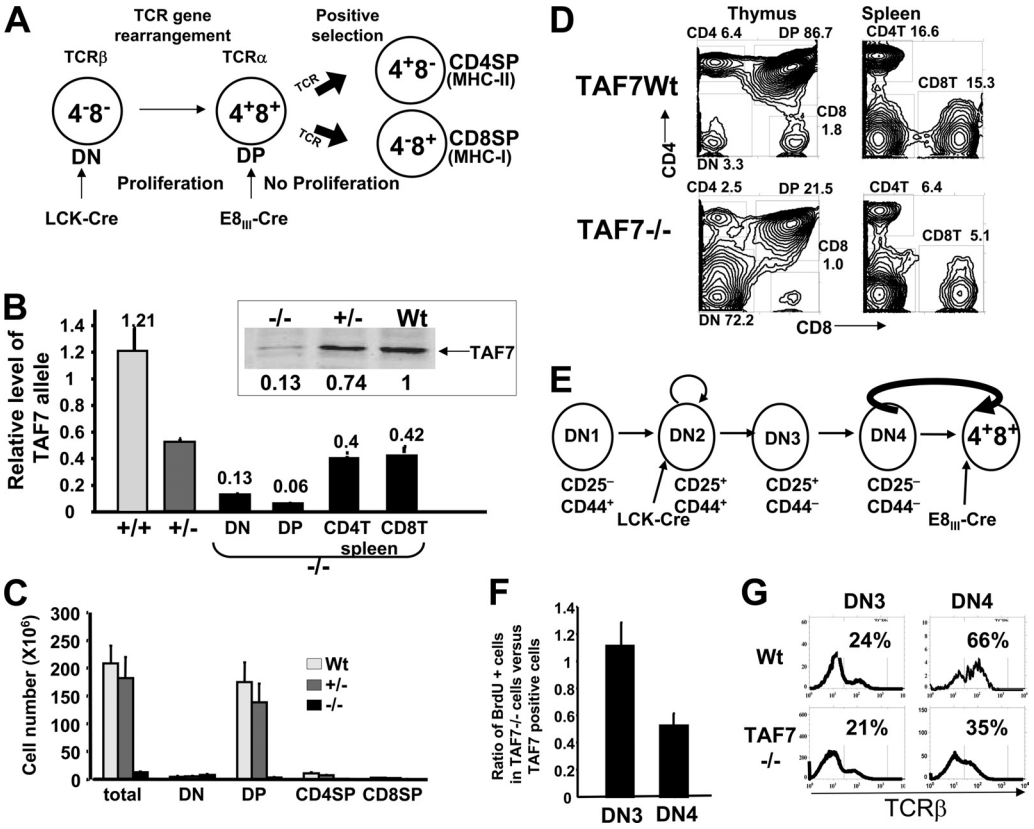

FIG 7 TAF7 is required early in thymic development. (A) Schematic representation of thymic differentiation. Immature thymocytes are $CD4^-$ $CD8^-$ double-negative (DN, 4^-8^-). During maturation, they rearrange the TCRβ gene, undergo massive proliferation, and express CD4 (abbreviated as "4") and CD8 (abbreviated as "8") receptor, becoming $CD4^+$ $CD8^+$ double positive (DP, 4^+8^+). After positive selection, DP thymocytes mature without proliferation, becoming either single positive CD4 (CD4 SP) or CD8 (CD8 SP) thymocytes. The LCK proximal promoter is active in DN thymocytes; the $E8_{III}$ promoter is active only in DP cells. (B) DN thymocytes from $TAF7^{f/-}$ LCK-Cre mice have deleted their TAF7 allele. Thymi and spleen were collected from Wt (+/+), $TAF7^{f/+}$ LCK-Cre ($TAF7^{+/-}$), and $TAF7^{f/-}$ LCK-Cre ($TAF7^{-/-}$) mice. DNA from purified DN and DP thymocytes and spleen CD4 and CD8 T cells was assayed by quantitative PCR for the extent of TAF7 deletion. The relative levels of TAF7 in each population is normalized to the level of the downstream neighboring gene, SLC25a2, which is not deleted (+/+, Control DNA). For the inset, protein extract was isolated from purified Wt, $TAF7^{f/+}$ LCK-Cre ($TAF7^{+/-}$), and $TAF7^{f/-}$ LCK-Cre ($TAF7^{-/-}$) DN thymocytes, and the TAF7 levels were determined by anti-TAF7 Western blotting. Relative protein levels were determined by densitometry and adjusted for input cell number. (C) Deletion of TAF7 at the DN stage dramatically blocks T cell development. Thymi were collected from $TAF7^{+/+}$ wild-type (Wt), $TAF7^{f/+}$ LCK-Cre ($TAF7^{+/-}$) heterozygous, and $TAF7^{f/-}$ LCK-Cre ($TAF7^{-/-}$) homozygous deletion mice. Thymocytes were classified as DN, DP, CD4 SP. or CD8 SP and quantified by flow cytometry based on CD4 and CD8 cell surface expression. The results represent the averages of independent analyses of seven $TAF7^{-/-}$ mice and seven litter-matched controls. The error bars represent the standard errors of the mean (SEM). (D) Most thymocytes in $TAF7^{-/-}$ thymi are DN. Thymi and spleens were collected from $TAF7^{+/+}$ Wt and $TAF7^{f/-}$ LCK-Cre ($TAF7^{-/-}$) mice; the cells were analyzed by flow cytometry for CD4 and CD8 expression. Indicated gates were used to quantify the distribution of cells. Spleen T cells were classified as CD4T and CD8T cells. Splenocytes staining for neither CD4 nor CD8 are non-T cells. (E) Schematic representation of the differentiation sequence of double-negative (DN) thymocytes. The stages of DN thymocyte differentiation are distinguished by the patterns of cell surface CD25 and CD44 markers. Limited thymocyte proliferation occurs at DN2 (narrow arced arrow); extensive proliferation occurs in DN4 to $CD4^+$ $CD8^+$ DP transition (wide arced arrow). The stages of thymocyte differentiation where the proximal LCK and $E8_{III}$ promoters are active are indicated. (F) Defective proliferation of $TAF7^{-/-}$ DN4 thymocytes. At 4 h after BrdU injection, DN3 and DN4 from Wt and $TAF7^{f/-}$ LCK-Cre ($TAF7^{-/-}$) mice were identified by flow cytometry based on CD44 and CD25 cell surface expression and analyzed for BrdU incorporation. The results are expressed as the ratio of $BrdU^+$ $TAF7^{-/-}$ thymocytes relative to $BrdU^+$ Wt thymocytes and represent the averages of three experiments. The error bars represent the SEM. (G) TCRβ expression is reduced in $TAF7^{-/-}$ DN4 cells. Thymi were collected from Wt and $TAF7^{f/-}$ LCK-Cre ($TAF7^{-/-}$) mice. DN3 and DN4 were stained for flow cytometry as described in Materials and Methods and fixed, and the TCRβ cytoplasmic expression was analyzed.

of DN thymocytes (DN1 to DN4) is not significantly different between TAF7-null and Wt mice (Fig. 7C), this raised the possibility that although TAF7 is required for thymocyte proliferation, it might not be required for their survival. To pursue this possibility, we examined the requirement for TAF7 during the transition of thymocytes from DP to SP cells, which does not depend on proliferation (Fig. 7A). To this end, $TAF7^{f/f}$ mice were crossed with $TAF7^{+/-}$ mice expressing Cre recombinase under the control of a CD8 enhancer/promoter ($E8_{III}$-Cre). The $E8_{III}$ promoter is functional only in preselection double-positive (DP) thymocytes (28). Thus, Cre expression from the $E8_{III}$ enhancer/promoter is transient and restricted to DP thymocytes; SP thymocytes are devoid of Cre (29). As shown in Fig. 8A, depletion of TAF7 beginning at the DP stage results in only a 40% reduction in the total thymocyte number, primarily reflecting the loss of DP thymocytes ($1 \times 10^8 \pm 0.1 \times 10^8$ in $TAF7^{-/-}$ mice versus $1.6 \times 10^8 \pm 0.3 \times 10^8$ in $TAF7^{+/-}$ mice), and a corresponding reduction in SP thymocytes ($5.5 \times 10^6 \pm 1.3 \times 10^6$ and $1.5 \times 10^6 \pm 0.2 \times 10^6$ in $TAF7^{-/-}$ mice versus 10 ± 2.2 and $3.0 \pm 0.5 \times 10^6$ in $TAF7^{+/-}$ mice, respectively). This is in contrast to the effect of TAF7 deple-

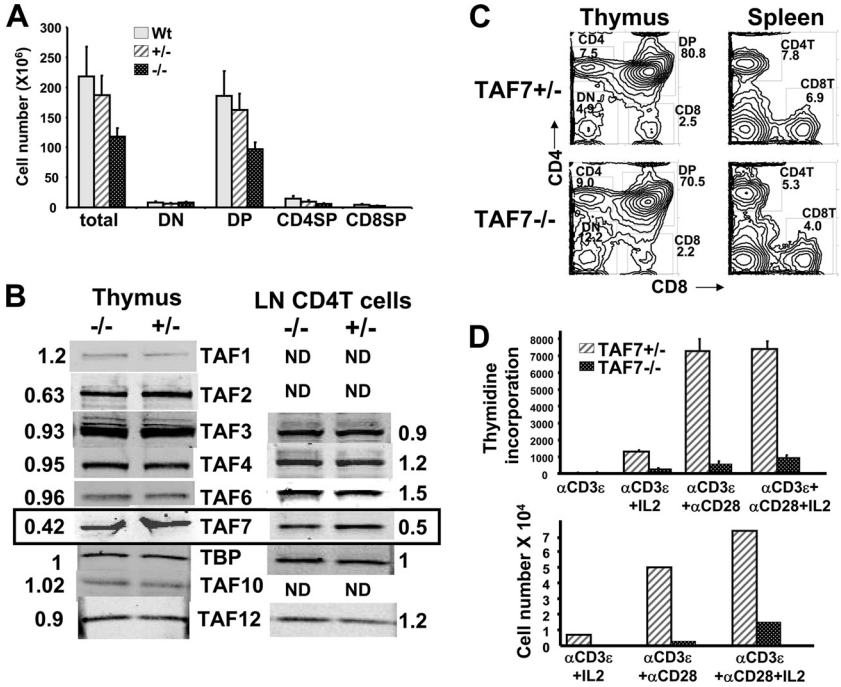

FIG 8 TAF7-null DP thymocytes differentiate and reach peripheral organs. (A) Deletion of TAF7 at the DP stage has a modest effect on T-cell development. Thymi were harvested from Wt, TAF7$^{f/+}$ E8$_{III}$-Cre (TAF7$^{+/-}$), and TAF7$^{f/-}$ E8$_{III}$-Cre (TAF7$^{-/-}$) mice (the E8$_{III}$ promoter is expressed only at the DP stage). Thymocytes were phenotyped and quantified by flow cytometry based on CD4 and CD8 cell surface expression. The results represent the averages of analyses of 10 TAF7$^{-/-}$ mice and an equal number of litter-matched controls. The error bars represent the SEM. (B) Deletion of TAF7 at the DP stage does not affect the level of expression of the other TAFs in thymocytes and CD4 naive T cells. The level of expression of different TFIID components was analyzed by Western blotting using soluble extracts either from thymocytes (left) or purified naive lymph node CD4 T cells (LN CD4T, right) collected from TAF7$^{f/+}$ E8$_{III}$-Cre (TAF7$^{+/-}$) and TAF7$^{f/-}$ E8$_{III}$-Cre (TAF7$^{-/-}$) mice as described in Materials and Methods. The relative abundances of different TFIID components were compared between −/− and +/− thymocytes and lymphocytes, corrected for the expression of the β-tubulin loading control, and expressed relative to the level of TBP (numbers on left and right sides). (C) TAF7$^{-/-}$ thymocytes give rise to mature single-positive thymocytes and peripheral T cells. Thymi and spleen were collected from TAF7$^{f/+}$ E8$_{III}$-Cre (TAF7$^{+/-}$) and TAF7$^{f/-}$ E8$_{III}$-Cre (TAF7$^{-/-}$) mice. Thymocytes were classified as DN, DP, CD4 SP, or CD8 SP, and T cells were classified as CD4T or CD8T cells and quantified by flow cytometry based on CD4 and CD8 cell surface expression. (D) TAF7-null T cells do not proliferate after *in vitro* stimulation. Lymph node CD4 T cells were purified from either TAF7$^{f/-}$ E8$_{III}$-Cre (−/−) or TAF7$^{f/+}$ E8III-Cre (+/−) mice and cultured in the presence of anti-CD3ε alone, anti-CD3ε with IL-2, anti-CD3ε and anti-CD28, or anti-CD3ε and anti-CD28 with IL-2. At 72 h, the cell proliferation was analyzed by [^{3}H]thymidine incorporation (top) and cell count (bottom). The top graph is the summary of three different experiments; the bottom graph is representative of two independent experiments. The error bars indicate the SEM.

tion at the DN stage, which decreased the number of DP thymocytes by 90%. Nevertheless, TAF7 protein is markedly depleted in the surviving thymocytes in TAF7$^{-/-}$ thymus, relative to the heterozygous TAF7$^{+/-}$ thymocytes (Fig. 8B). Surprisingly, the number of single positive thymocytes is not disproportionately affected, despite the deletion of TAF7 at the DP stage and the distribution of thymocyte subpopulations indistinguishable between the TAF7$^{-/-}$ and TAF7$^{+/-}$ mice (Fig. 8C, left panel), indicating that loss of TAF7 does not significantly alter differentiation from DP to SP thymocyte. These findings suggest that TAF7 is critically required for DN proliferation is but not required for further differentiation.

TAF7 is not required for the differentiation of SP thymocytes. To pursue the possibility that TAF7 is not required for the survival of single-positive (SP) thymocytes or their differentiation into mature, peripheral T cells, we examined the T-cell populations in lymph nodes of TAF7$^{f/-}$ E8$_{III}$-Cre mice. Remarkably, although the total number of T cells was reduced in the lymph nodes of the TAF7$^{f/-}$ E8$_{III}$-Cre (TAF7$^{-/-}$) mice (5×10^7 in TAF7$^{-/-}$ mice versus 1.05×10^8 in TAF7$^{+/-}$ mice, respectively), both CD4 and CD8 T cells were recovered. Although the absolute numbers of CD4 and CD8 T cells were lower than in lymph nodes from heterozygotes (11.6×10^6 and 7.3×10^6 in TAF7$^{-/-}$ mice versus 39×10^6 and 33×10^6 in TAF7$^{+/-}$ mice, respectively), the ratio between CD4 and CD8 T cells was similar to the one observed in control TAF7$^{+/-}$ mice (Fig. 8C, right panel). Importantly, both CD4 and CD8 T-cell subpopulations derived from TAF7$^{f/-}$ E8$_{III}$-Cre (TAF7$^{-/-}$) mice were markedly depleted of TAF7 protein, relative to the TAF7$^{+/-}$ control (Fig. 8B and data not shown). Since the extent of TAF7 depletion in lymph node CD4 T cells is not different from that in the thymus, this suggests that DP thymocytes depleted of TAF7 are not at a selective disadvantage in differentiating to CD4 T cells, relative to TAF7-depleted cells (Fig. 8B, data not shown). (Intracellular staining and flow cytometry revealed a bimodal distribution of cells completely negative for TAF7 and those cells that were TAF7 positive that had escaped deletion [data not shown].) Thus, TAF7 is not required for the differentiation and survival of mature T cells or their emergence from the thymus into the periphery.

TAF7 depletion in either thymocytes or lymph node T cells did not affect either the absolute or relative abundances of the other TFIID components in (Fig. 8B). Thus, the maturation of T cells is not accompanied by a change in TFIID composition, as has been reported in other systems (12, 11).

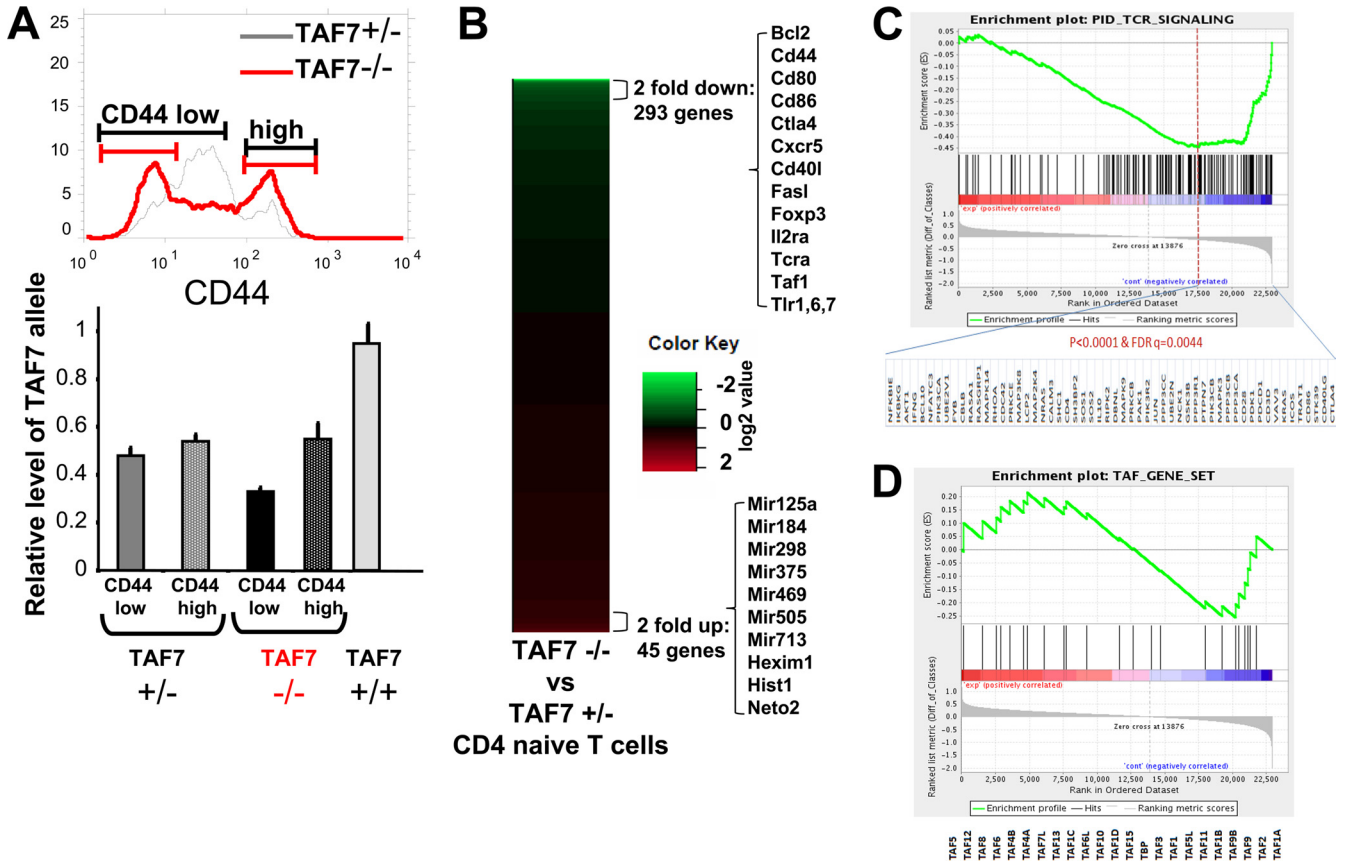

FIG 9 TAF7 deletion in peripheral naive CD4 T cells affects only a small subset of genes. (A) TAF7 is deleted in naive, CD44^{low} CD4 T cells but not in memory, CD44^{high} CD4 T cells. (Top) CD4 naive and memory T cells were purified from the spleens of TAF7$^{f/-}$ E8$_{III}$-Cre (−/−) and TAF7$^{f/+}$ E8$_{III}$-Cre (+/−) mice by FACS. Red and black brackets indicate the cell populations used to determine the extent of TAF7 deletion. The CD44^{low} populations from either TAF7$^{f/-}$ E8$_{III}$-Cre (−/−) or TAF7$^{f/+}$ E8$_{III}$-Cre (+/−) mice were used in panel B. (Bottom) The extents of TAF7 gene deletion in purified CD4 naive and memory T cells from either TAF7$^{f/-}$ E8$_{III}$-Cre (−/−) or TAF7$^{f/+}$ E8$_{III}$-Cre (+/−) mice determined by quantitative PCR and normalized relative to the neighboring downstream gene, SLC25a2, which is not deleted. (B) Deletion of TAF7 affects the expression of only a very small subset on transcripts in naive, CD44^{low} CD4 T cells. Total RNA was purified from naive CD44^{low} CD4 T cells (indicated in panel A) from either TAF7$^{f/-}$ E8$_{III}$-Cre (−/−) or TAF7$^{f/+}$ E8$_{III}$-Cre (+/−) mice, and transcript levels were determined by hybridization on an Affymetrix Mouse Gene 1.0 ST array. The heatmap represents the $\log_2$ ratio of the signal intensity of the knockout (−/−) relative to the heterozygote (+/−), where the value of the heterozygote is set to 0 for each point. Indicated on the right are some of the few transcripts affected by TAF7 deletion. (C) Enrichment plot of TCR signaling pathway. TCR signaling is significantly downregulated in TAF7$^{-/-}$ mice ($P < 0.0001$). The green curve shows the running sum of enrichment score (ES) for ranked genes. The red vertical line specifies the maximum ES score. The genes listed under the plot are the leading edge subset which accounts for the gene set's enrichment signal. (D) Enrichment plot of TAF_GENE_SET. The TAF_gene_set is not enriched. TAF genes are shown in both up- and downregulation.

TAF7-null T cells do not expand after stimulation. Since peripheral T cells proliferate in response to antigenic stimulation, we next determined whether TAF7-deficient peripheral T cells were capable of stimulation and expansion. Lymph node T cells from either TAF7$^{f/-}$ E8$_{III}$-Cre (TAF7$^{-/-}$) or TAF7$^{f/+}$ E8$_{III}$-Cre (TAF7$^{+/-}$) mice were stimulated *in vitro* with either anti-CD3ε or a combination of anti-CD3ε and anti-CD28 antibodies. Their capacity to proliferate was assessed both by incorporation of [^{3}H]thymidine and by direct cell count (Fig. 8D, top and bottom, respectively). Whereas control TAF7$^{+/-}$ T cells undergo massive proliferation and expansion upon stimulation, TAF7-null T cells do neither, either in the absence or in the presence of IL-2 (Fig. 8D). The few T cells from lymph nodes of TAF7$^{-/-}$ mice that were recovered after stimulation did not have TAF7 deleted, suggesting that the only T cells able to proliferate upon stimulation were those that had escaped deletion (data not shown).

To pursue this observation, the TAF7 status of naive and memory CD4 T cells in the spleens of TAF7$^{f/-}$ E8$_{III}$-Cre was examined. The conversion of naive to memory T cells (as defined by the expression of CD44) requires proliferation. Naive (CD44^{low}) and memory (CD44^{high}) splenic T cells were purified from TAF7$^{f/-}$ E8$_{III}$-Cre (TAF7$^{-/-}$) mice, and the extent of TAF7 deletion was analyzed by quantitative PCR (Fig. 9A). Only the naive CD44^{low} T cells, not the memory CD44^{high} T cells, have TAF7 deleted, indicating that proliferation of peripheral T cells *in vivo* requires TAF7.

We conclude that TAF7 is necessary for early thymocyte survival and/or proliferation but is not required for the survival or differentiation of mature T cells or their egress from the thymus. TAF7 is required again for peripheral T cells to proliferate in response to antigenic stimulation.

TAF7 deletion affects a small number of genes in naive CD4 T cells. Since TAF7$^{-/-}$ T cells survive in the periphery but are not able to proliferate upon stimulation, we next determined what

effect TAF7 deletion has on gene expression by comparing the expression profiles of purified naive CD4 T cells from $TAF7^{f/-}$ $E8_{III}$-Cre ($TAF7^{-/-}$) or $TAF7^{f/+}$ $E8_{III}$-Cre ($TAF7^{+/-}$) mice (Fig. 9B). As expected, TAF7 expression is significantly reduced in naive CD4 $TAF7^{-/-}$ T cells compared to heterozygous controls (32%). Surprisingly, only a small number of genes are affected by TAF7 deletion (Fig. 9B). Of the approximately 25,000 transcripts that were detected on the arrays, at most 639 were altered by TAF7 depletion. Of these, the majority ($n = 510$) were downregulated and included components of the TCR signaling pathway (Fig. 9B and C), a finding consistent with the failure of TAF7-null T cells to respond to stimulation. The upregulated transcripts ($n = 129$) included a large number of microRNAs. As assessed by GSEA, a number of TAF transcripts are affected, displaying both enrichment and depletion (Fig. 9D), although TAF proteins and TFIID are still present in these cells (Fig. 8B). Among the transcripts that are not affected by TAF7 depletion are those encoding ribosomal proteins, glycolysis/gluconeogenesis, RNA processing, translation, and the metabolism/electron chain transport pathways. Therefore, whereas TAF7 deletion in immature cells (i.e., MEFs) has a global effect on transcription, its deletion in differentiated naive T cells affects only a subset of genes related to T-cell function.

DISCUSSION

Early studies of transcription led to the model that general transcription factors, such as TFIID, that interact with the core promoter are common to all RNA Pol II-dependent transcription and essential for transcription. The present studies challenge that perspective. As we report here, whereas TAF7 is essential for cell survival and proliferation during early embryogenesis and differentiation, it is not critical for later stages of T-cell differentiation in the thymus.

These findings extend other recent studies suggesting that significant regulatory events occur at the core promoter. For example, different core promoter structures are associated with different gene subfamilies: Inr or ATG desert promoters more commonly subserve constitutively expressed genes, whereas TATA core promoters more often are contained within tissue-specific genes (30). Importantly, different cell types differ in their requirement for general transcription factors. For example, it has been reported that during the differentiation of myoblasts to myocytes, multiple TFIID components, including TBP, are lost (12). Similarly, the requirement for TAFs changes during hepatocyte development (11). Cell type-specific requirements for TAFs, such as TAF10, have been reported in other systems (20, 25, 35). Even at a single core promoter, the requirements for general transcription factors change in response to transcriptional signals. As we have shown, constitutive MHC class I gene transcription depends on the TFIID component TAF1, whereas gamma interferon-activated transcription of both MHC class I and class II genes bypasses the requirement for TAF1 and depends instead on the coactivator CIITA (37). More recently, we have reported that the TFIID component, TAF7, acts as a "checkpoint regulator" of MHC class I transcription initiation through its interactions with TAF1, CIITA, TFIIH, and P-TEFb (14). Despite its critical role in regulating MHC class I transcription, TAF7 does not have a global effect on transcription in 293 kidney cells (3). Taken together, these findings suggested that the requirements for general transcription factors, and TAF7 in particular, may differ among different cell types.

Our findings have shown that TAF7 is required for survival and proliferation during embryonic development. Germ line deletion of TAF7 is embryonic lethal, with death occurring by between 3.5 and 5.5 dpc at the time of implantation and proliferation (34). Although $TAF7^{-/-}$ embryos are able to hatch and elicit a decidual response, they die coincident with the proliferative expansion of embryonic and extraembryonic tissues and implantation. It remains to be determined whether $TAF7^{-/-}$ embryonic development until 4.5 dpc is independent of TAF7 or supported by maternal TAF7. However, the essentiality of TAF7 at this very early developmental stage is consistent with the presence of TAF7 mRNA and protein in Wt 3.5-dpc blastocysts and its expression in both trophoblast and inner cell mass (ICM) cells (39).

TAF7 continues to be important later in embryonic development for the survival and proliferation of embryonic cells. Depletion of TAF7 in MEFs, derived from 13.5-dpc embryos, results in a global cessation of RNA polymerase II-dependent transcription. Within 3 days of TAF7 depletion, MEF cultures cease expanding and begin to die. The few $TAF7^{-/-}$ cells remaining after 8 days of culture undergo senescence, as measured by SA β-galactosidase staining. Interestingly, neither cell death nor senescence occurs by typical mechanisms, likely reflecting the absence of TAF7-dependent gene products that may be involved in those processes.

TAF7 also is required for the differentiation and proliferation of immature thymocytes. Thymocyte differentiation from the immature DN stage to the DP stage requires both rearrangement of the TCRβ gene and a burst of proliferation (4). TAF7 deletion at the DN stage arrests proliferation and further development to the DP stage. Although TCRβ expression occurs, it is at a reduced level that likely reflects the activity of residual TAF7. Taken together, these data indicate that TAF7 regulates the genes involved in the proliferation and differentiation of early thymocytes.

Unexpectedly, deletion of TAF7 does not prevent differentiation that occurs independently of proliferation. TAF7 depletion in DP thymocytes, does not prevent positive selection and further differentiation into SP thymocytes nor their maturation into T cells and migration into peripheral lymph nodes. T-cell maturation beyond the DP stage requires a series of molecular events, including the *de novo* expression of IL-7R, ThPOK, and CCR7 genes in $CD4^+$ cells. The present findings indicate that these transcriptional events in T-cell maturation can occur without TAF7 and that naive $TAF7^{-/-}$ T cells survive in peripheral lymphoid organs. However, peripheral naive T cells that did not depend on TAF7 for either differentiation or thymic egress, reacquire their dependence on TAF7 for their expansion after antigenic stimulation. In contrast to hepatocyte or myotube differentiation, where the TFIID complex in immature cells is replaced by alternative complexes in the mature cells, the TFIID complex persists during T cell differentiation, although the requirement for TAF7 changes, a finding consistent with TAF7 function beyond TFIID, as a regulator of transcription initiation (13).

These studies challenge the prevailing perspective that the TFIID complex is static in composition and function. They emphasize the fact that different TAFs affect distinct cellular pathways and differentiation programs. TAF7, like TAF8 and TAF10, is required in the very early stages of development. In contrast, TAF4 does not appear to be required before 9.5 dpc of mouse embryogenesis (24) (although some of its functions might be sub-

sumed by its paralog TAF4b). We have demonstrated previously that TAF7 functions as a regulator of transcription initiation, modulating the enzymatic activities of the transcription factors necessary for preinitiation complex formation, initiation and elongation, including P-TEFb, TFIIH, and CIITA (13). Although TAF7 functions broadly as a regulator of Pol II gene transcription in MEFs, it only affects a subset of genes in mature T cells. The transcriptional mechanisms that support the acquisition of TAF7 independence during differentiation will be the focus of future investigations.

ACKNOWLEDGMENTS

We thank Remy Bosselut, Richard Hodes, Dave Levens, and Brian Lewis for critical reading of the manuscript, Li Wang, Manuella Pellegrini, and Lionel Feigenbaum for their advice in the generation and maintenance of the knockout lines, and Jeremy Daniel and Valeria Orlova for helpful discussions. We also thank Susan Sharrow, Tony Adams, and Larry Granger for help with the flow cytometry studies.

This study was supported by the Intramural Research Program of the U.S. National Institutes of Health, the National Cancer Institute and the Center for Cancer Research.

A.G. generated and performed all of the biological analyses of the TAF7KO mice. X.T. prepared lymph node T cells and helped with experiments. J.Z., G.W., C.C., Q.-R.C., Z.Y., and D.M. performed the microarray hybridizations and data analysis. J.Z., A.Y., J.H., J.R.-C., and S.M. assisted with the embryological and laser capture microscopy technology and analysis. T.G. and K.H. provided assistance and guidance on analyses of thymocyte differentiation and lineage commitment. D.S., K.B., and A.S. helped design, analyze, and interpret experiments.

REFERENCES

1. **Amsterdam A, Hopkins N.** 1999. Retrovirus-mediated insertional mutagenesis in zebrafish. Methods Cell Biol. **60**:87–98.
2. **Amsterdam A, et al.** 2004. Identification of 315 genes essential for early zebrafish development. Proc. Natl. Acad. Sci. U. S. A. **101**:12792–12797.
3. **Ballachanda DN, et al.** 2010. Novel functions for TAF7, a regulator of TAF1-independent transcription. J. Biol. Chem. **285**:38772–38780.
4. **Bosselut R.** 2004. CD4/CD8-lineage differentiation in the thymus: from nuclear effectors to membrane signals. Nat. Rev. Immunol. **4**:529–540.
5. **Casse C, Giannoni F, Nguyen VT, Dubois MF, Bensaude O.** 1999. The transcriptional inhibitors, actinomycin D and alpha-amanitin, activate the HIV-1 promoter and favor phosphorylation of the RNA polymerase II C-terminal domain. J. Biol. Chem. **274**:16097–16106.
6. **Cheng Y, et al.** 2007. Abnormal sperm in mice lacking the Taf7l gene. Mol. Cell. Biol. **27**:2582–2589.
7. **Choukrallah MA, et al.** 2012. Interconversion between active and inactive TATA-binding protein transcription complexes in the mouse genome. Nucleic Acids Res. **40**:1446–1459.
8. **Cler E, Papai G, Schultz P, Davidson I.** 2009. Recent advances in understanding the structure and function of general transcription factor TFIID. Cell. Mol. Life Sci. **66**:2123–2134.
9. **Collado M, Serrano M.** 2006. The power and the promise of oncogene-induced senescence markers. Nat. Rev. Cancer **6**:472–476.
10. **Court DL, et al.** 2003. Mini-lambda: a tractable system for chromosome and BAC engineering. Gene **315**:63–69.
11. **D'Alessio JA, Ng R, Willenbring H, Tjian R.** Core promoter recognition complex changes accompany liver development. Proc. Natl. Acad. Sci. U. S. A. **108**:3906–3911.
12. **Deato MD, Tjian R.** 2007. Switching of the core transcription machinery during myogenesis. Genes Dev. **21**:2137–2149.
13. **Gegonne A, et al.** 2008. TFIID component TAF7 functionally interacts with both TFIIH and P-TEFb. Proc. Natl. Acad. Sci. U. S. A. **105**:5367–5372.
14. **Gegonne A, Weissman JD, Zhou M, Brady JN, Singer DS.** 2006. TAF7: a possible transcription initiation check-point regulator. Proc. Natl. Acad. Sci. U. S. A. **103**:602–607.
15. **Gegonne A, et al.** 2001. TAFII55 binding to TAFII250 inhibits its acetyltransferase activity. Proc. Natl. Acad. Sci. U. S. A. **98**:12432–12437.
16. **Golling G, et al.** 2002. Insertional mutagenesis in zebrafish rapidly identifies genes essential for early vertebrate development. Nat. Genet. **31**:135–140.
17. **Grant PA, et al.** 1998. A subset of TAF(II)s are integral components of the SAGA complex required for nucleosome acetylation and transcriptional stimulation. Cell **94**:45–53.
18. **Guermah M, Ge K, Chiang CM, Roeder RG.** 2003. The TBN protein, which is essential for early embryonic mouse development, is an inducible TAFII implicated in adipogenesis. Mol. Cell **12**:991–1001.
19. **Hogan BL.** 1994. Developmental signaling: sorting out the signals. Curr. Biol. **4**:1122–1124.
20. **Indra AK, et al.** 2005. TAF10 is required for the establishment of skin barrier function in fetal, but not in adult mouse epidermis. Dev. Biol. **285**:28–37.
21. **Kolthur-Seetharam U, Martianov I, Davidson I.** 2008. Specialization of the general transcriptional machinery in male germ cells. Cell Cycle. **7**:3493–3498.
22. **Lee PP, et al.** 2001. A critical role for Dnmt1 and DNA methylation in T cell development, function, and survival. Immunity **15**:763–774.
23. **Liu P, Jenkins NA, Copeland NG.** 2003. A highly efficient recombineering-based method for generating conditional knockout mutations. Genome Res. **13**:476–484.
24. **Mengus G, et al.** 2005. TAF4 inactivation in embryonic fibroblasts activates TGFβ signaling and autocrine growth. EMBO J. **24**:2753–2767.
25. **Mohan WS, Jr, Scheer E, Wendling O, Metzger D, Tora L.** 2003. TAF10 ($TAF_{II}30$) is necessary for TFIID stability and early embryogenesis in mice. Mol. Cell. Biol. **23**:4307–4318.
26. **Muller F, Demeny MA, Tora L.** 2007. New problems in RNA polymerase II transcription initiation: matching the diversity of core promoters with a variety of promoter recognition factors. J. Biol. Chem. **282**:14685–14689.
27. **Muller F, Zaucker A, Tora L.** 2010. Developmental regulation of transcription initiation: more than just changing the actors. Curr. Opin. Genet. Dev. **20**:533–540.
28. **Ogryzko VV, et al.** 1998. Histone-like TAFs within the PCAF histone acetylase complex. Cell **94**:35–44.
29. **Park JH, et al.** 2010. Signaling by intrathymic cytokines, not T cell antigen receptors, specifies CD8 lineage choice and promotes the differentiation of cytotoxic-lineage T cells. Nat. Immunol. **11**:257–264.
30. **Schug J, et al.** 2005. Promoter features related to tissue specificity as measured by Shannon entropy. Genome Biol. **6**:R33.
31. **Schwartz LB, Sklar VE, Jaehning JA, Weinmann R, Roeder RG.** 1974. Isolation and partial characterization of the multiple forms of deoxyribonucleic acid-dependent ribonucleic acid polymerase in the mouse myeloma, MOPC 315. J. Biol. Chem. **249**:5889–5897.
32. **Shen W, et al.** 2003. Systematic analysis of essential yeast TAFs in genome-wide transcription and preinitiation complex assembly. EMBO J. **13**:3395–3402.
33. **Sims RJ, III, Belotserkovskaya R, Reinberg D.** 2004. Elongation by RNA polymerase II: the short and long of it. Genes Dev. **18**:2437–2468.
34. **Tam PP, Loebel DA.** 2007. Gene function in mouse embryogenesis: get set for gastrulation. Nat. Rev. Genet. **8**:368–381.
35. **Tatarakis A, et al.** 2008. Dominant and redundant functions of TFIID involved in the regulation of hepatic genes. Mol. Cell **31**:531–543.
36. **Voss AK, et al.** 2000. Taube nuss is a novel gene essential for the survival of pluripotent cells of early mouse embryos. Development **127**:5449–5461.
37. **Weissman JD, Howcroft TK, Singer DS.** 2000. TAFII250-independent transcription can be conferred on a TAFii250-dependent basal promoter by upstream activators. J. Biol. Chem. **275**:10160–10167.
38. **Wieczorek E, Brand M, Jacq X, Tora L.** 1998. Function of TAF(II)-containing complex without TBP in transcription by RNA polymerase II. Nature **393**:187–191.
39. **Yoshikawa T, et al.** 2006. High-throughput screen for genes predominantly expressed in the ICM of mouse blastocysts by whole mount in situ hybridization. Gene Expr. Patterns **6**:213–224.